Journal of Nuclear Materials 378 (2008) 30–34

Contents lists available at ScienceDirect

Journal of Nuclear Materials

journal homepage: www.elsevier.com/locate/jnucmat

Delayed hydride cracking of spent fuel rods in dry storage

Young Suk Kim *

Zirconium Team, Korea Atomic Energy Research Institute, 150, Dukjin-dong, Yuseong, Daejeon 305-353, Republic of Korea

ARTICLE INFO

Article history:
Received 16 October 2007
Accepted 5 April 2008

PACS:
81. 40.Np

ABSTRACT

Failures of zirconium alloy cladding tubes during a long-term storage at room temperature were first reported by Simpson and Ells in 1974, which remains unresolved by the old delayed hydride cracking (DHC) models. Using our new DHC model, we examined failures of cladding tubes after their storage at room temperature. Stress-induced hydride phase transformation from γ to δ at a crack tip creates a difference in hydrogen concentration between the bulk region and the crack tip due to a higher hydrogen solubility of the γ-hydride, which is a driving force for DHC at low temperatures. Accounting for our new DHC model and the failures of zirconium alloy cladding tubes during long-term storage at room temperature, we suggest that the spent fuel rods to be stored either in an isothermal condition or in a slow cooling condition would fail by DHC during their dry storage upon cooling to below 180 °C. Further works are recommended to establish DHC failure criterion for the spent fuel rods that are being stored in dry storage.

1. Introduction

Dry storage of spent fuel rods is being considered as an alternative to the interim storage method until a final decision on their final disposal is made [1]. Most studies on the integrity of spent fuel rods in dry storage have focused on cladding creep, which is known to be the most likely failure mechanism [2,3], and reorientation of hydrides to secure their retrievability after dry storage [4]. Little attention has been paid to delayed hydride cracking (DHC) because this phenomenon will not occur due to limited stresses and slow diffusion of hydrogen at low temperatures below 200 °C [3,5]. However, Simpson and Ells reported a failure of unirradiated Zr–2.5Nb fuel rods after their long-term storage at room temperature, the cause of which was recognized to be DHC [6]. Therefore, it is clear that in contrast to what is believed to be that no DHC occurs in the spent fuel rods in dry storage, they would fail as long as stress raisers such as surface flaws or the weld region are present inside the cladding tube. Especially, high burnup fuel rods may have incipient cracks on the inside cladding surface due to an interaction of the fuel and the cladding during reactor operation [4]. Three instances of spent fuel rod failures were also reported where a leakage occurred less than 2 months after the spent fuel rods were stored at rather low temperatures below 275 °C [2,7]. Although the cause of their failures is unknown, these failures have shown that the incipient cracks present inside them grow fast to through-wall cracks in the spent fuel rods even at low temperatures, because the leakage has occurred within 2 months after the start of their dry storage. Thus, we suggest that these failures of the spent fuel rods are likely due to DHC, the rationale of which is given in this study. The aim of this study is to demonstrate the DHC susceptibility of spent fuel rods by citing Simpson and Ells's results [6] and to provide a rationale for the failures of spent fuel rods due to DHC even at room temperature using our new DHC model [8–11], which remains unclear to date.

2. A model for delayed hydride cracking (DHC) at low temperatures

Although the old DHC models suggest that a driving force for DHC is a stress gradient, they cannot provide a rationale for DHC of zirconium alloys with the test temperature approached by heating. It should be noted that when the bulk region of zirconium alloys has the hydrogen concentration in solution corresponding to the terminal solid solubility for dissolution (TSSD) or C_{TSSD} (point A in Fig. 1) due to an approach to the test temperature by heating, the hydrogen concentration at the crack tip cannot reach the terminal solid solubility for precipitation (TSSP) or C_{TSSP} (point A′ in Fig. 1) even under tensile stresses applied to the crack tip [12–15]. In other words, according to the old DHC models where hydrides are precipitated upon an increase in the hydrogen concentration at the crack tip to C_{TSSP} (point A′), DHC could not have occurred in zirconium alloys charged to several tens to hundreds ppm of hydrogen with the test temperature approached by heating. This explains why no DHC occurs in furnace-cooled zirconium alloys with hydrogen at the test temperatures above 180 °C upon an approach by heating [15]. However, at low temperatures below 180 °C, DHC occurs despite the test temperature being approached

* Tel.: +82 42 868 2359; fax: +82 42 868 8346.
E-mail address: yskim1@kaeri.re.kr

0022-3115/$ - see front matter © 2008 Elsevier B.V. All rights reserved.
doi:10.1016/j.jnucmat.2008.04.011

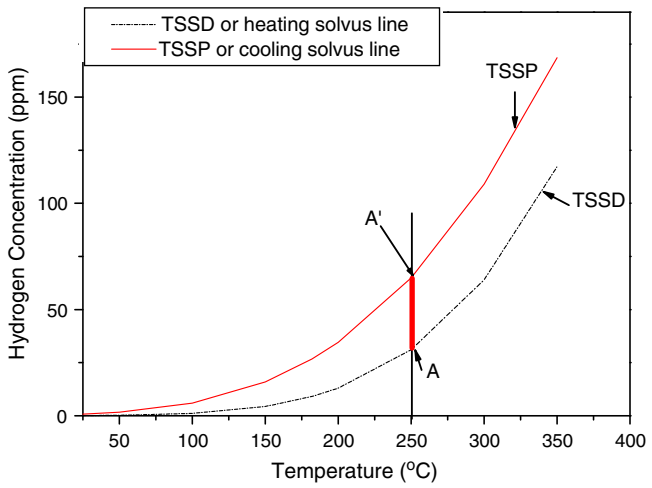

Fig. 1. The hydrogen solvus that a crack tip can reach at 250 °C due to tensile stresses in isothermal conditions, according to the old DHC models, when the hydrogen concentration in the bulk region of a zirconium alloy tube corresponds to TSSD (point A) by an approach by heating from below [9–12].

by heating as demonstrated by Kim et al. [10], Ambler [15] and Huang et al. [16].

According to our new DHC model [8–11], however, a driving force for DHC is the hydrogen concentration gradient at a crack tip, arising from the stress-induced precipitation of hydrides or stress-induced hydride phase transformation from γ to δ. Especially, with the test temperature approached by heating or in isothermal conditions, the specimens have the hydrogen concentration in solution corresponding to C_{TSSD} (point A in Fig. 1), which is the same between the crack tip and the bulk region. In this case, the stress-induced precipitation of the hydrides cannot occur due to no supersaturation of hydrogen. However, when the test temperature is below the γ- to δ-hydride phase transformation temperature, corresponding to 182 °C for furnace-cooled zirconium alloys [17] or 255 °C for water-quenched ones [18], γ-hydrides are precipitated in addition to δ-hydrides in the bulk region of the zirconium alloys [17]. In contrast, at stress raisers such as surface flaws or cracks, only the δ-hydrides are precipitated due to the stress-induced hydride phase transformation from γ to δ, causing different distributions of the hydrides between the bulk region and the crack tip: a mixture of the γ- and δ-hydrides in the bulk region and only the δ-hydrides at the stress raisers such as the surface flaws or cracks. Experimental evidence is provided by examining the hydride distribution between the fracture surface and the bulk region, 20 mm away from that, in a Zr–2.5Nb compact tension specimen with 60 ppm H after a DHC test at 250 °C. As shown in Fig. 2 [10], only the δ-hydrides were observed on the fracture surfaces but in the bulk region, the γ-hydrides were found. Ambler also made a similar comment that the hydrides precipitated at the crack tip would be the δ-hydrides [15]. Different distributions of the hydrides between the bulk region and the crack tip, as shown in Fig. 2, cause a difference in hydrogen solvus between them due to a higher hydrogen solubility of the γ-hydrides compared to that of the δ-hydrides as schematically shown in Fig. 3. In other words, the bulk region has a higher concentration of hydrogen in solution due to the presence of the γ-hydrides than the crack tip with the δ-hydrides only, creating the difference in hydrogen concentration or ΔC between them which is a driving force for DHC in isothermal conditions or when the test temperature is approached by heating. The ΔC would correspond to the distance CC′ for the water-quenched zirconium alloys or the distance C_1C' for the furnace-cooled ones, as shown in Fig. 3. Experimental evidence for a higher hydrogen solubility of the γ-hydrides is provided by comparing the measured solubility data of the γ-hydrides reported by Cann and Atrens [19], Mishra and Asundi [20] and Carpenter and Watters [21] with that of the δ-hydride [22], as shown in Fig. 4. Here, the ΔC corresponds to the distance AA′ for the water-quenched zirconium alloys and the distance BB′ for the furnace-cooled ones, as shown in Fig. 4. Nath et al. also made a similar suggestion that the solvus temperatures of the δ-hydride would be higher than those of the γ-hydrides based on the nucleation behavior of each hydride with the temperature [23]. Other evidence for a higher solubility of the γ-hydrides

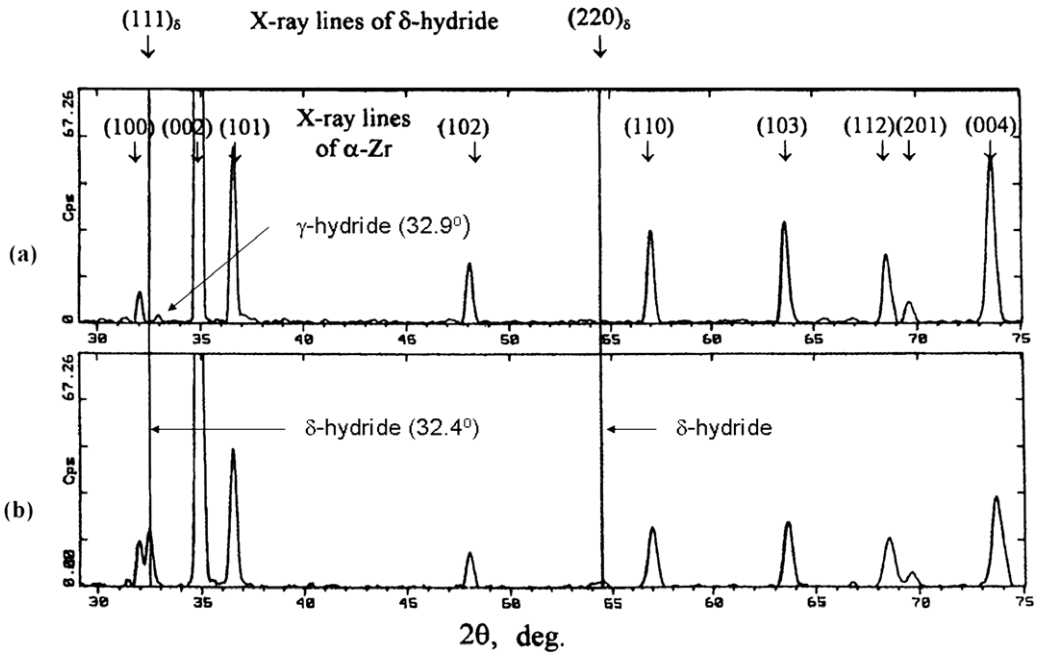

Fig. 2. X-ray diffraction analyses of (a) the bulk region at a distance of 20 mm from the crack tip and of (b) the crack tip in the water-quenched Zr–2.5Nb specimens subjected to a DHC test at 250 °C.

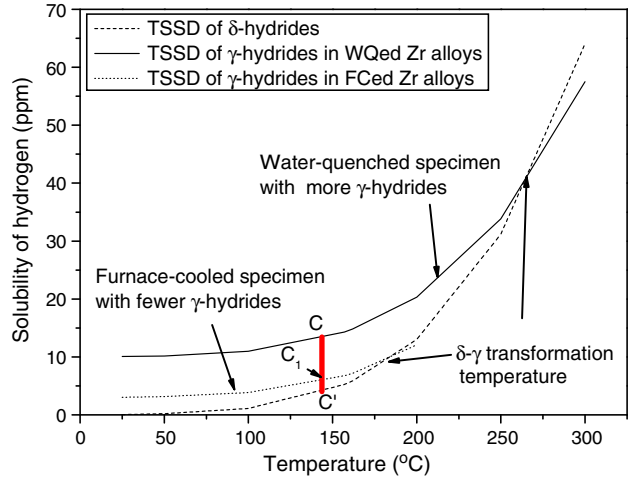

Fig. 3. Diagram schematically illustrating the heating solvus (or terminal solid solubility) of the Zr–2.5Nb specimens that depends on the cooling rate, the hydride phase and the concentration of the γ-hydride, creating the ΔC between the crack tip and the bulk region corresponding to the distance CC′ or C_1C'.

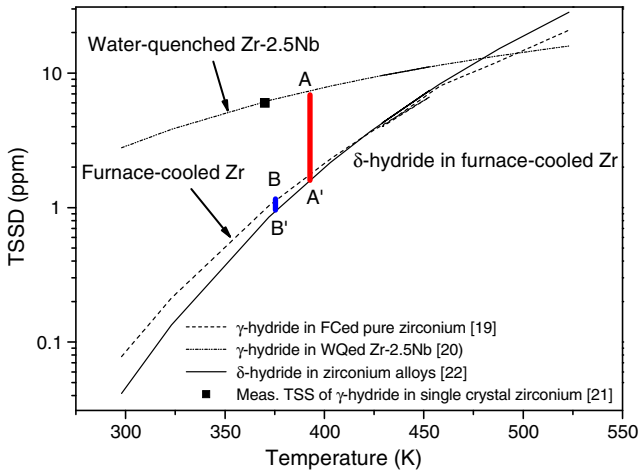

Fig. 4. Measured terminal solid solubility of the γ-hydride in the furnace-cooled zirconium (Cann [19]) and in the water-quenched Zr–2.5Nb alloy (Mishra [20]) and of the δ-hydride determined from Kearns data [22] along with the measured TSS of the γ-hydride in water-quenched zirconium single crystal (Carpenter[21]): the ΔC corresponds to the distance AA′ for the water-quenched zirconium alloys or the distance BB′ for the furnace-cooled ones.

is provided by the experimental facts demonstrating two different activation energies for the cooling solvus of hydrogen (or terminal solid solubility for precipitation (TSSP)): a lower activation energy below 260 °C and a higher activation energy above it [24]. Considering that the total strain energy of the γ-hydrides is smaller than that of the δ-hydride [13,15], a change in the slope of the cooling solvus line, as reported in the literature [17,24–25] corresponds to precipitation of the γ-hydrides besides the δ-hydrides in the zirconium matrix. The temperature corresponding to the inflection point of the slope strongly depends on the cooling rate: 260 °C for a higher cooling rate of 10 °C/min [24] and 170 °C for a slower cooling rate of 2 °C/min [25]. Given that the δ- to γ-hydride phase transformation temperatures in zirconium alloys are 182 °C for the furnace-cooled Zr–2.5Nb tubes [17] and 255 °C for the water-quenched zirconium [18], it is obvious that this inflection point of the slope of the cooling solvus line corresponds to the onset of precipitation of the γ-hydrides.

More direct evidence for a higher hydrogen solubility of the γ-hydride is provided by Root and Fong's experiment [17] where the

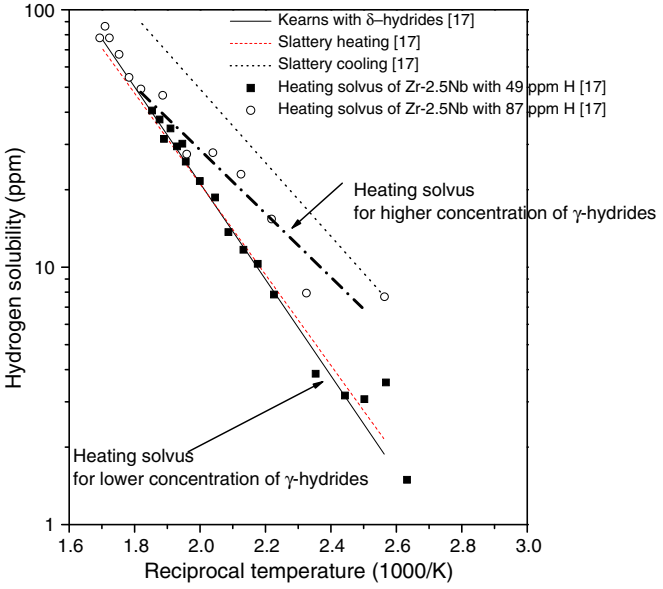

Fig. 5. Heating solvus of the Zr–2.5Nb specimens with 49 and 87 ppm H, respectively that were determined by neutron diffraction [17], demonstrating that the Zr–2.5Nb specimen with 87 ppm H had higher solubility of hydrogen due to a higher concentration of the γ-hydride when compared to that with 49 ppm H.

specimen with 87 ppm H had a higher hydrogen solubility on heating than that with 49 ppm H whose hydrogen solubility fell on the Kearns solvus line, as shown in Fig. 5. It should be remembered that since the specimens have been stored for 2 years after charging of hydrogen [18], the concentration of the γ-hydride would increase with time even at room temperature due to the hydride phase transformation from δ to γ [26]. Consequently, a higher hydrogen solubility of the specimen with 87 ppm H on heating (Fig. 5), when compared to that of the specimen with 49 ppm H falling on the Kearns solvus line, is likely due to the increased concentration of the γ-hydride with a higher hydrogen solubility.

Accounting for all the experimental results shown above, accordingly, we conclude that the stress induced hydride phase transformation from γ to δ causes the ΔC between the bulk region and the stress raisers such as cracks, causing hydrogen to move from the bulk region to a crack tip in zirconium alloys even in isothermal conditions or in slow cooled conditions. Furthermore, this can explain why DHC of a Zr–2.5Nb tube occurs with little cooling from the terminal solid solubility for dissolution (TSSD) temperature below 180 °C, as shown in Fig. 6 on cooling from 50 °C above the TSSD temperatures [12]. It should be noted that at the test temperatures above 180 °C, DHC initiation has occurred with some degree of undercooling from the TSSD temperatures, corresponding to the distance AB shown in Fig. 6. Conversely, when the test temperature is higher than the δ- to γ-hydride phase transformation temperatures, for example, 182 °C for the furnace-cooled Zr–2.5Nb tube, no DHC occurs on approaching the test temperature by heating due to no δ- to γ-hydride phase transformation: for examples, when the test temperature of 250 °C was approached by heating, no DHC occurred in a Zr–2.5Nb tube specimen (Fig. 7). In contrast, the water-quenched Zr–2.5Nb tube specimens had DHC even at 250 °C when approached by heating, as shown in Fig. 7, due to the δ- to γ-hydride phase transformation. This occurs because the γ hydrides are present even at 250 °C in the water quenched specimens given that the hydride phase transformation temperature for the water-quenched specimen is higher than the test temperature, as shown in Fig. 4. Conclusively, our new DHC model demonstrates that DHC occurs at low temperatures below 180 °C due to the δ- to γ-hydride phase transformation in zirconium

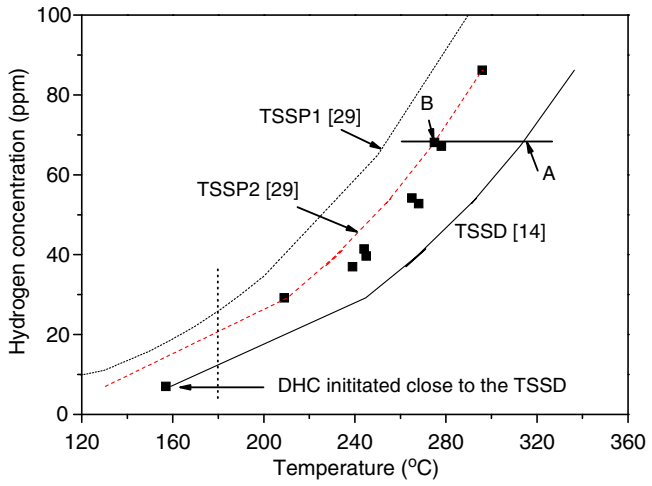

Fig. 6. DHC initiation temperatures with hydrogen concentrations of the unirradiated Zr–2.5Nb tube when cooled from 50 °C above the terminal solid solubility for dissolution (TSSD) temperatures. When the test temperature was lowered to below 180 °C, DHC initiation occurred closed to the TSSD temperature [12,29].

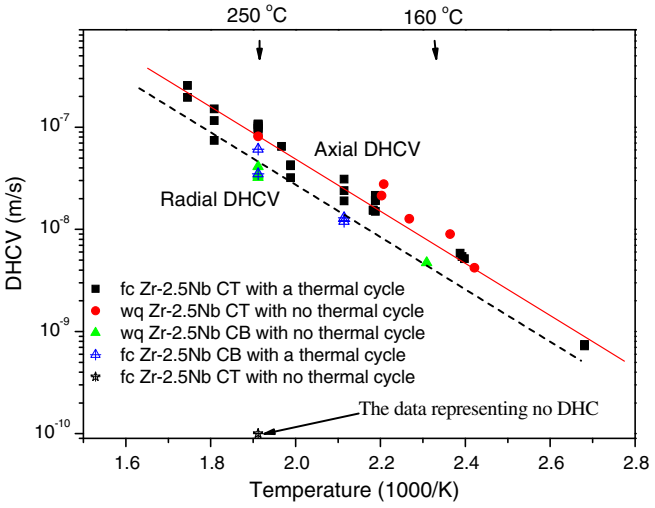

Fig. 7. Axial and radial delayed hydride cracking velocity (DHCV) of the water-quenched and furnace-cooled Zr–2.5Nb specimens with and without a thermal cycle that were determined by using compact tension (CT) and cantilever beam (CB) specimens, respectively. On approaching the test temperature by heating, the furnace-cooled Zr–2.5Nb had no DHC at 250 °C at which the water-quenched Zr–2.5Nb had DHC [10].

alloys with hydrogen such as spent fuel rods if the stress raisers such as a surface flaw or the weld region of high tensile stresses exist.

3. Failures of spent fuel rods at low temperatures by DHC

Simpson and Ells [6] showed that for a Zr–2.5Nb cladding tube containing only 10 ppm of hydrogen the hydrides were precipitated at room temperature at the root of the end cap weld 4 weeks after welding and then a crack grew there to about 90% of the cladding wall thickness (equal to 0.41 mm) 2 years after that. A simple calculation assuming the growth of a crack to be 0.9 times the thickness over 2 years shows that the crack growth rate was at the least 5.9×10^{-12} m/s, which is over 10^4 times faster than the predicted crack growth rate, 1.6×10^{-16} m/s [6], by the old DHC models. Then, they conducted another verification test using the cladding tube with 100 ppm H where a faster growing crack with time was also observed at the same place or the root of the end cap weld [6]. When a Vickers microhardness impression was made in a Zr–2.5Nb alloy sheet charged to 100–300 ppm H, the hydrides at each of the corners of the microhardness impression that did not exist a few minutes after that impression were observed six months after that, causing a crack growth there by their cracking [6]. Given that the microhardness impression tests had been conducted at room temperature, it is obvious that DHC occurs in zirconium alloy with hydrogen even at room temperature if a stress raiser is present, which cannot be satisfactorily understood by the old DHC models.

Precipitation of the hydrides and subsequent crack growth by their cracking in cladding tubes of zirconium alloys even at room temperature as described above is similar to the cases where DHC occurs at 250 °C for the water-quenched Zr–2.5Nb tube when approached by heating as shown in Fig. 7 or initiates near the TSSD temperature with little undercooling when cooled from 50 °C above the TSSD as shown in Fig. 6. A driving force for cracking of zirconium alloy cladding tubes at room temperature is the ΔC caused by the δ- to γ-hydride phase transformation, corresponding to the distance AA′ or BB′ shown in Fig. 4: the bulk region containing the δ- and γ-hydrides with a higher hydrogen solubility and the weld region containing δ-hydrides only with a lower hydrogen solubility. Considering that the γ-hydrides are precipitated at low temperatures below 182 °C for the slow cooled zirconium alloys such as the spent fuel rods, it is not until the spent fuel rods are cooled to below 180 °C that DHC occurs due to stress-induced hydride phase transformation from γ to δ. We can estimate when the cladding temperatures of the spent fuel rods become lower than 180 °C using Einziger's method for predicting temperature of a fuel assembly [27]. Fig. 8 shows an example of the fuel assembly temperature predicted by Einziger's method. Assuming that the cladding temperature is conservatively similar to the average temperature of the fuel assembly, it takes at least 30 years for the cladding temperatures to completely fall to below 180 °C (Fig. 8). This estimation is in line with Sasahara's prediction that more than 30 years of the cooling time is needed to cool the cladding temperatures of spent fuel rods to below 180 °C [28]. In other words, even though a visual inspection of the spent fuel rods after dry storage of 15–20 years showed little evidence of DHC [27,28], it is too early to draw concrete conclusions about the DHC effect on

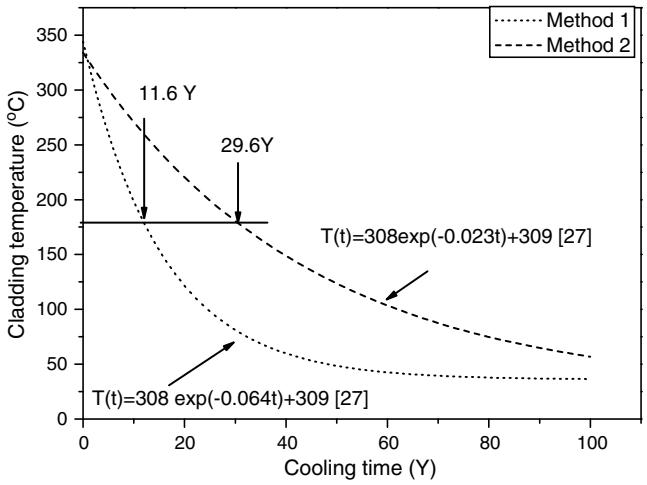

Fig. 8. Estimated temperatures of a fuel assembly during dry storage period depending on the methods to develop a temperature profile for calculating creep deformation for the storage period: for the 1st method, the profile was fixed at 617 K at the start of storage and 428 K at 14.8 years and for the 2nd method, the temperature is assumed to be proportional to the exponentially decreasing decay heat until the ambient temperature dominated [27].

the integrity of spent fuel rods. It is not until the storage time exceeds 30 years that DHC is activated, likely causing a leakage from the spent fuel rods. Other evidence for this hypothesis is provided by the failures of the spent fuel rods that had been stored at relatively low temperatures below 275 °C [7].

4. Conclusions

Failures of unirradiated Zr-2.5 cladding tubes occurred even at room temperature due to cracking of the hydrides precipitated at stress raisers such as the weld region. These facts demonstrate that DHC occurs even at room temperature in zirconium alloys with hydrogen, only if stress raisers are present. Consequently, it is concluded that the spent fuel rods to be stored in dry storage would fail due to this low temperature DHC only if they have stress raisers inside the cladding surface. Given that this phenomenon occurs only after cooling the cladding temperatures of the spent fuel rods to below the γ- to δ-hydride phase transformation temperature, it is not until 30 years have passed that failures of the spent fuel rods by DHC would occur. The driving force for this low temperature DHC is a difference in hydrogen concentration between the bulk region and the crack tip arising from stress-induced hydride phase transformation from γ to δ, which is evidenced by a higher hydrogen solubility of the γ-hydrides when compared to that of the δ-hydrides. Further works are recommended to establish DHC failure criterion for the spent fuel rods that are being stored in dry storage.

Acknowledgements

This work has been carried out under the Nuclear R&D Program supported by Ministry of Education Science and Technology (MEST), Korea.

References

[1] E.W. Brach, Interim Staff Guidance-11. Rev. 3. Cladding considerations for the transportation and storage of spent fuel, US Nuclear Regulatory Commission, Spent Fuel Project Office, Rockville, MD, 2003.
[2] M.E. Cunningham, E.P. Simonen, R.T. Allemann, I.S. Levy, R.F. Hazolton, PNL 6364 (1987).
[3] M. Peehs, F. Garzarolli, W. Goll, IAEA-TECDOC-1089, Vienna 1999, p. 313.
[4] R.E. Einziger, C.L. Brown, G.P. Hornseth, C.G. Interrante, Radwaste Solutions (2005) 44. March/April.
[5] IAEA-TECDOC-1293, Long Term Storage of Spent Nuclear Fuel-Survey and Recommendations, Final Report of a Co-ordinated Research Project 1994–1997, International Atomic Energy Agency, 2002.
[6] C.J. Simpson, C.E. Ells, J. Nucl. Mater. 52 (1974) 289.
[7] International Atomic Energy Agency, Extended storage of spent fuel, IAEA-TECDOC-673, 1992.
[8] Y.S. Kim, Metals Mater. Int. 11 (2005) 29.
[9] Y.S. Kim, S.B. Ahn, Y.M. Cheong, J. Alloys Compd. 429 (2007) 221.
[10] Y.S. Kim, K.S. Kim, Y.M. Cheong, J. Nucl. Sci. Technol. 43 (2006) 1120.
[11] Y.S. Kim, Mater. Sci. Eng. A 468–470 (2007) 281.
[12] Y.S. Kim, S.B. Ahn, Y.M. Cheong, ASME Pressure Vessel and Piping 2006/11th 2006 International Conference on Pressure Vessel Technology, Vancouver, 2006, PVP2006-ICPVT11-94062.
[13] M.P. Puls, Acta Metall. 32 (1984) 1259.
[14] S.Q. Shi, G.K. Shek, M.P. Puls, J. Nucl. Mater. 218 (1995) 189.
[15] J.F.R. Ambler, in: Proceedings of the 6th International Symposium on Zirconium in the Nuclear Industry, ASTM STP 824, ASTM, 1984, p. 653.
[16] F.H. Huang, W.J. Mills, Met. Mater. Trans. 22A (1991) 2049.
[17] J.H. Root, R.W.L. Fong, J. Nucl. Mater. 232 (1996) 75.
[18] S. Mishra, K.S. Sivaramakrishnan, M.K. Asundi, J. Nucl. Mater. 45 (1972) 235.
[19] C.D. Cann, A. Atrens, J. Nucl. Mater. 88 (1980) 42. 1980.
[20] S. Mishra, M.M. Asundi, in: Zirconium in nuclear applications, ASTM STP 551, American Society for Testing and Materials, 1974, p. 63.
[21] G.J.C. Carpenter, J.F. Watters, J. Nucl. Mater. 73 (1978) 190.
[22] J.J. Kearns, J. Nucl. Mater. 22 (1967) 292.
[23] B. Nath, G.W. Lorimer, N. Ridley, J. Nucl. Mater. 49 (1973) 262.
[24] K. Une, S. Ishimoto, J. Nucl. Sci. Technol. 41 (2004) 949.
[25] A. McMinn, E.C. Darby, J.S. Schofield, in: Proceedings of the 12th Symposium on Zirconium in the Nuclear Industry, ASTM STP 1354, ASTM, 2000, p. 173.
[26] J.H. Root, W.M. Small, D. Khatamian, O. Woo, Acta Mater. 51 (2003) 2042.
[27] R.E. Einziger, H. Tsai, M. Billone, Nucl. Technol. 144 (2003) 186.
[28] A. Sasahara, T. Matsumura, Nucl. Eng. Design 238 (2008) 1250.
[29] Z.L. Pan, I.G. Ritchie, M.P. Puls, J. Nucl. Mater. 228 (1996) 227.